Available online at www.sciencedirect.com
SCIENCE DIRECT
International Journal of Heat and Fluid Flow 27 (2006) 585–593
International Journal of HEAT AND FLUID FLOW
www.elsevier.com/locate/ijhff

A synthetic-eddy-method for generating inflow conditions for large-eddy simulations

N. Jarrin [a,*], S. Benhamadouche [b], D. Laurence [a], R. Prosser [a]

[a] School of Mechanical, Aerospace and Civil Engineering, The University of Manchester, Manchester, UK
[b] Département Mécanique des Fluides et Transferts Thermiques, Electricité de France, Chatou, France

Available online 30 March 2006

Abstract

The generation of inflow data for spatially developing turbulent flows is one of the challenges that must be addressed prior to the application of LES to industrial flows and complex geometries. A new method of generation of synthetic turbulence, suitable for complex geometries and unstructured meshes, is presented herein. The method is based on the classical view of turbulence as a superposition of coherent structures. It is able to reproduce prescribed first and second order one point statistics, characteristic length and time scales, and the shape of coherent structures. The ability of the method to produce realistic inflow conditions in the test cases of a spatially decaying homogeneous isotropic turbulence and of a fully developed turbulent channel flow is presented. The method is systematically compared to other methods of generation of inflow conditions (precursor simulation, spectral methods and algebraic methods).

Keywords: Large-eddy simulation; Synthetic turbulence; Inflow boundary conditions; Spatially decaying isotropic turbulence; Channel flow

1. Introduction

It is widely accepted that the specification of realistic inlet boundary conditions play a major role in the accuracy of a numerical simulation. For RANS approaches, only mean profiles for the velocity and the turbulence variables need to be prescribed, which makes the definition of inflow data comparatively straight-forward. For large-eddy and direct-numerical simulations, the generation of inflow data is much more of an issue. The early applications of LES were simple temporally developing flows where the simulation generated its own inflow data using periodic boundary conditions. With the progress of the computer powers, LES has been increasingly used to simulate spatially developing flows, which require the specification of instantaneous turbulent inlet boundary conditions. From an engineering point of view, almost all flows of industrial interest are spatially evolving flows. The need for methods to generate realistic unsteady inflow conditions is then mandatory to use LES in industrial cases with a certain degree of confidence in the results. It has been shown that the results of DNS or LES, particularly in the cases of a plane jet (Klein et al., 2003), a spatially developing boundary layer (Lund et al., 1998) or a backward facing step (Jarrin et al., 2003) are very sensitive to upstream inflow conditions.

The most accurate technique to impose the inlet boundary conditions of a LES consists of obtaining inflow data from a precursor simulation. The inflow represents exactly the large scale eddies of the flow at the inlet and there is no or very little transient downstream the inlet. This technique has two major drawbacks. Firstly, it is restricted to simple cases where the flow at the inlet of the computational domain can be regarded as a fully developed turbulent flow (Kaltenbach et al., 1999) or a spatially developing turbulent boundary layer (Lund et al., 1998) and therefore lacks generality. In the scope of performing embedded LES or hybrid RANS/

* Corresponding author. Tel.: +44 161 200 3730; fax: +44 161 200 3723.
E-mail addresses: n.jarrin@postgrad.manchester.ac.uk (N. Jarrin), sofiane.benhamadouche@edf.fr (S. Benhamadouche), dominique.laurence@manchester.ac.uk (D. Laurence), robert.prosser@manchester.ac.uk (R. Prosser).

0142-727X/$ - see front matter © 2006 Elsevier Inc. All rights reserved.
doi:10.1016/j.ijheatfluidflow.2006.02.006

LES, this approach is not suitable either. Secondly, it entails a heavy extra computational load and requires important storage capacities. Thus the research effort seems to head towards methods of generation of synthetic turbulence which can be both faster and more flexible. These methods try to generate an inflow signal which is as close as possible to the real flow by matching a reduced set of statistics. The statistics typically available are the mean velocity, the turbulent kinetic energy, the dissipation rate and sometimes the full Reynolds stress tensor profiles.

A basic technique to generate turbulent inflow data is to take a mean velocity profile with superimposed random fluctuations. The data generated do not exhibit any spatial or temporal correlations. The energy generated is also uniformly spread over all wave numbers and, due to a lack of large scale energy-containing structures, the pseudo turbulence is quickly dissipated (Jarrin et al., 2003).

A standard method to give some spatial and temporal correlations to the generated data is to create time series of velocity fluctuations by performing an inverse Fourier transform for prescribed spectral densities (Lee et al., 1992 or Kondo et al., 1997). The amplitude of the Fourier modes are computed from the model spectrum and their phase is drawn randomly. The missing phase information of the real turbulent eddies makes these methods less accurate than the ones employing a precursor simulation and a transition section downstream of the inlet is necessary for the flow to become realistic again. The main objective of methods of generation of synthetic turbulence is to reduce this transition section to be able to use shorter domains and hence reduce the cost of the simulation. Even though these methods were applied with success for the simulation of both isotropic homogeneous turbulence (Lee et al., 1992) and flow over a backward facing-step (Le et al., 1997), they have several drawbacks which make them unsuitable for industrial purposes. Indeed they are derived to generate periodic signals on uniform meshes. It is not clear if a Fourier decomposition of the inflow signal can be used in the case of non-homogeneous turbulence, or at least it does not have any justification. On complex unstructured inlet meshes where the fast Fourier transform cannot be used, they become expensive and hence not appropriate. Adaptations of these spectral methods able to tackle industrial issues have been proposed by Smirnov et al., 2001) and then Batten et al. (2004). These authors use different spectra rescaled by some turbulent variables at different locations across the flow and limit the number of modes simulated to reduce the computational cost of generation of the inflow data. Keating et al. (2004) noted that on the plane channel flow at $Re^* = 400$ the method of Batten et al. (2004) produces a transition region downstream of the inlet of about 20 channel half height before the flow becomes fully turbulent.

Another family of techniques for arbitrary inlet meshes is to filter random data on the inlet mesh (Klein et al., 2003). Gaussian filters have been used to generate inflow data with spatial and temporal correlations. An advantage of this method is that it is particularly suitable for non-homogeneous turbulence and complex inlet meshes as the size of the filter can easily be varied across the flow. Unfortunately it can become very expensive as the mesh is refined.

To obtain more insight into the flow physics, Druault et al. (2004) used a proper-orthogonal-decomposition of a turbulent signal coming from an external source and used this signal as an inflow condition for LES calculation. Even though this technique cannot be applied systematically for general flows as it requires a previous realization of the flow, it is interesting to note that a better simulation of the large scale coherent structures of the flow at the inlet enables a better simulation of the downstream flow.

The idea behind the method presented in this paper is to directly focus on prescribing coherent structures rather than reverting to spectral methods. It is a generalisation of the previous work of Jarrin et al. (2003) which used streamwise vortices to trigger turbulence downstream of the inlet in an LES calculation. The method presented herein is easy to implement, fast to run and performs well on any geometry and any kind of flow. The data generated exhibit very good physical properties such as; first and second order one point statistics, prescribed length scales, time scales and the shape of the autocorrelation function.

2. Numerical procedure

2.1. Inflow generation method

The method is based on the classic view of turbulence as a superposition of coherent structures. Coherent structures will be generated over the inlet plane of our calculation and will be defined by a shape function that encompasses the structure's spatial and temporal characteristics.

We start with the one-dimensional case, where a one component velocity signal is to be generated on the interval $[a,b]$. $f_\sigma(x)$ is the shape function of the turbulent spot, which has a compact support on $[-\sigma,\sigma]$ and satisfies the normalization condition

$$\frac{1}{\Delta}\int_{-\Delta/2}^{\Delta/2} f_\sigma^2(x)\mathrm{d}x = 1 \tag{1}$$

where $\Delta = b - a + 2\sigma$. Each turbulent spot i has a position x_i (defining its physical location) and a length scale σ_i (defining its spectral content). For the sake of simplicity, we retain a constant σ_i for the moment. The issue of non-constant length scale σ will be tackled later. Each spot is assigned a sign ε_i. Thus the contribution $u^{(i)}(x)$ of turbulent spot i to the velocity field is

$$u^{(i)}(x) = \varepsilon_i f_\sigma(x - x_i) \tag{2}$$

where ε_i is a random step of value $+1$ or -1 and x_i is drawn randomly on the interval $[a-\sigma,\ b+\sigma]$. The synthetic eddies are generated on an interval larger than $[a,\ b]$ so that the boundary points can be surrounded by eddies. The

velocity signal at a point x is the sum of the contribution of all synthetic eddies on the domain. For N eddies it reads

$$u(x) = \frac{1}{\sqrt{N}} \sum_{i=1}^{N} \varepsilon_i f_\sigma(x - x_i) \tag{3}$$

The number of eddies on the domain can be set to $(b-a)/\sigma$ which ensures that the plane remains statistically covered with turbulent spots.

It can readily be shown then that our signal is of zero mean, unit variance and that the two-point autocorrelation function reads

$$R_{uu}(r) = \frac{1}{\Delta} \int_{-\Delta/2}^{\Delta/2} f_\sigma(x) f_\sigma(x+r) \mathrm{d}x \tag{4}$$

Thus inflow data with any autocorrelation function can be generated. However inverting Eq. (4) to obtain f_σ from R_{uu} involves performing a complex deconvolution procedure. Details of such a procedure can be found in di Mare and Jones (2005). Herein the simpler approach of choosing f_σ a priori is chosen.

The generalisation of the 1D procedure to the generation of 2D time dependent fluctuations is straight-forward. The eddies are now three-dimensional structures with compact three-dimensional supports on $[-\sigma_x, \sigma_x; -\sigma_y, \sigma_y; -\sigma_z, \sigma_z]$, satisfying a three-dimensional normalization condition of the same type as Eq. (1). The inlet plane is located at $x = 0$ and it has dimensions $[0, L_z] \times [0, L_y]$. The position (x_i, y_i, z_i) of synthetic-eddy i is drawn randomly on $[-\sigma_x, \sigma_x] \times [-\sigma_y, L_y + \sigma_y] \times [-\sigma_z, L_z + \sigma_z]$. The eddies are convected through the inlet plane with a reference velocity scale U_0 using Taylor's frozen turbulence hypothesis $x_i(t + \mathrm{d}t) = x_i(t) + U_0 \mathrm{d}t$. Once $x_i(t) > \sigma_x$ the eddy is regenerated upstream at $x = -\sigma_x$ and convected again through the inlet plane. The signal at a point $\underline{x}$ and a time t in the inlet flow plane reads

$$u'_j(\underline{x}, t) = \frac{1}{\sqrt{N}} \sum_{i=1}^{N} \varepsilon_{ij} f_j(\underline{x} - \underline{x}_i(t)) \tag{5}$$

where ε_{ij} is the sign of vortex i on component j and are independent random steps of values $+1$ or -1. The number of turbulent spots N on the inlet plane can be approximated by S_p/S_s where S_p is the surface of the inlet plane and S_s the surface of the support of a turbulent spot, which ensures the inlet plane remains statistically covered with synthetic eddies.

The independence of the rotation sign ensures that our inflow signal satisfies the condition $\overline{u_i u_j} = \delta_{ij}$. If the Reynolds stress tensor R_{ij} and the mean velocity profile $\overline{u_i}$ are known a priori from previous experiments, DNS or RANS calculations, our signal can be transformed to match these statistics (Lund et al., 1998). The final velocity field u_i is then reconstructed from the vortex field u'_i according to

$$u_i = \overline{u_i} + a_{ij} u'_j \tag{6}$$

where a_{ij} is obtained from the prescribed Reynolds stress tensor and reads

$$\begin{pmatrix} \sqrt{R_{11}} & 0 & 0 \\ R_{21}/a_{11} & \sqrt{R_{22} - a_{21}^2} & 0 \\ R_{31}/a_{11} & (R_{32} - a_{21}a_{31})/a_{22} & \sqrt{R_{33} - a_{31}^2 - a_{32}^2} \end{pmatrix} \tag{7}$$

The length scale in the flow can also be varied. This is clearly one advantage of our method compared to spectral methods. The compact support of the spots enables us to have different length scales in different parts of the flow which might be of great interest to simulate wall flows. However, it must be mentioned that a strong variation of the length scale leads to a deviation of the correlation function from the analytical formulae Eq. (4) which assumes constant length scales. Further distortions can result from the rescaling procedure Eq. (6), but are normally small (Smirnov et al., 2001). The structures of the flow can also be controlled, for instance to generate streamwise vortices in the near wall layer of a channel while more isotropic eddies are imposed at the center. In the following, the method will thus be referred to as the synthetic-eddy-method (SEM). Only simple turbulent spots with a Gaussian decay of the intensity of the spots are going to be considered hereafter. In this case, the shape function of the synthetic-eddy reads

$$f_j(\underline{x}) = f(\|\underline{x}\|) \tag{8}$$

where f is a Gaussian function.

2.2. Flow solver

Code_Saturne, a collocated finite volume code for complex geometries (Archambeau et al., 2004) and (Benhamadouche and Laurence, 2003) is used to solve the incompressible Navier–Stokes equations. Velocity and pressure coupling is ensured by a prediction/correction method with a SIMPLEC algorithm. The collocated discretization requires a Rhie and Chow (1982) interpolation in the correction step to avoid oscillatory solutions. A second order centered scheme (in space and time) is used.

3. Spatially decaying isotropic turbulence

The mean flow is in the positive x direction. The mesh dimensions are $6\pi \times 2\pi \times 2\pi$, respectively, in the x, y and z directions. The mesh is homogeneous in all three directions and has $192 \times 64 \times 64$ cells. Periodic boundary conditions are used in the y and z direction. The Smagorinsky constant is set to its theoretical value $C_S = 0.18$.

The independent parameters defining the calculation are the mean streamwise velocity $U_0 = 20$ m/s, the viscosity $\nu = 3.5 \times 10^{-4}$ m^2/s, the turbulent energy $k = 3/2$ m^2/s^2 and the integral length scale L defined as the distance at which the two-point correlation has the value 0.01. The first three parameters are kept constant which leaves only one free parameter, the length scale L that defines the Reynolds number. Simulations carried out using different length scales and different methods are listed in Table 1. The time step is $\mathrm{d}t = \mathrm{d}x/U_0$. Statistics are averaged over

Table 1
Computations for the spatially decaying isotropic turbulence case

Case	Method	Details
RAND	Basic random	X
DIG0	Digital filtering	Gaussian filter, $L = 0.4$
SPE0	Spectral method	$k^2 e^{-(k/k_0)^2}$ spectrum, $L = 0.4$
SEM0	SEM	Gaussian spots, $L = 0.4$
SEM1	SEM	Gaussian spots, $L = 0.2$
SEM2	SEM	Gaussian spots, $L = 0.8$

two flow-through domain time and over the y and z directions.

The results obtained using a basic random procedure RAND, the synthetic-eddy-method SEM0, the digital filtering technique of Klein et al. (2003) DIG0 and the spectral method of Lee et al. SPE0 are first compared. SEM0 uses 3D isotropic turbulent spots with a Gaussian decay of the spots (Eq. (8)). The synthetic eddies are convected by the mean flow U_0. DIG0 uses Gaussian filters. SPE0 uses an isotropic energy spectrum of the form $(k^2 \exp(-k^2/k_0^2)$. The size of the structures in SEM0, SPE0 and DIG0 can be controlled so that the three methods produce inflow data with the same correlations and energy spectrum (Fig. 1). SEM0, SPE0 and DIG0 thus only differ by the procedure chosen to generate the inflow data. It can be seen on Fig. 2 that the theoretical value of the skewness is reached after the same distance downstream of the inlet for SEM0, SPE0 and DIG0 and that the turbulent energy decays at similar rates. The large eddy turn-over time scale (LETOT) evaluated as $T = L/u' = 0.4$ s ($L = 0.4$ m, $u' = 1$ m/s) corresponds to a convection distance of $x = 8$ m ($U_0 = 20$ m/s). Thus the skewness is established after one LETOT. The kink on all k profiles from $x = 0$ to $x = 0.5$ is most certainly a numerical artifact but not linked to incompressibility (even divergence-free structures generate a similar kink).

RAND does not recover the correct skewness even by the end of the domain and all the energy is dissipated after a few cells downstream the inlet. The inflow data does not have any spatial or temporal correlation. Two neighbouring points are uncorrelated, which leads to high velocity gradients and high dissipation. The energy cascade does not establish as there is too much energy in the high wavenumber part of the spectrum and the skewness without energy transfer cannot converge towards its theoretical value for the case. On Fig. 3, the evolution of the one-dimensional longitudinal energy spectrum confirms this interpretation. SEM0 has too little energy at high wavenumber due to the Gaussian decay of the spots and energy is cascaded from the low wavenumber part of the spectrum to the high wavenumber part. On the contrary, RAND has too much energy at high wavenumbers and this energy is dissipated. The spectra in both RAND and SEM0 tend towards a classic filtered 5/3 spectrum for LES.

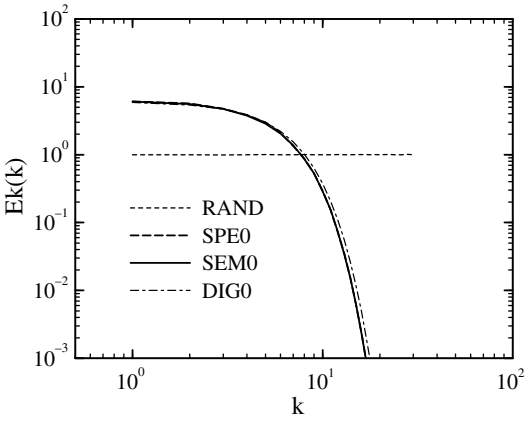

Fig. 1. One-dimensional longitudinal energy spectrum of the inflow data for spatially decaying isotropic turbulence.

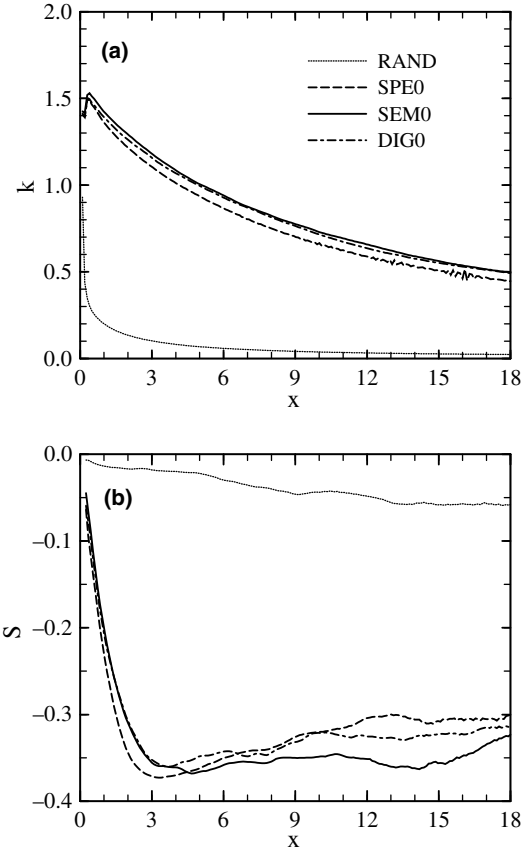

Fig. 2. Downstream evolution of the (a) turbulent kinetic energy and (b) velocity derivative skewness for the spatially decaying isotropic turbulence.

Different sizes of turbulent spots are now generated at the inlet. Calculations SEM1 has inflow fluctuations with turbulent spots twice smaller than SEM0, whereas SEM2 has turbulent spots twice bigger than SEM0. The one-dimensional longitudinal energy spectrum of SEM0, SEM1, SEM2 and RAND is given on Fig. 4. These different spectra produce inflow data with different values of the dissipation at the inlet. The bigger the spots are, the lower the dissipation is and the slower the decay of the turbulent kinetic energy is as $dk/dt = -\varepsilon$. As smaller spots are gener-

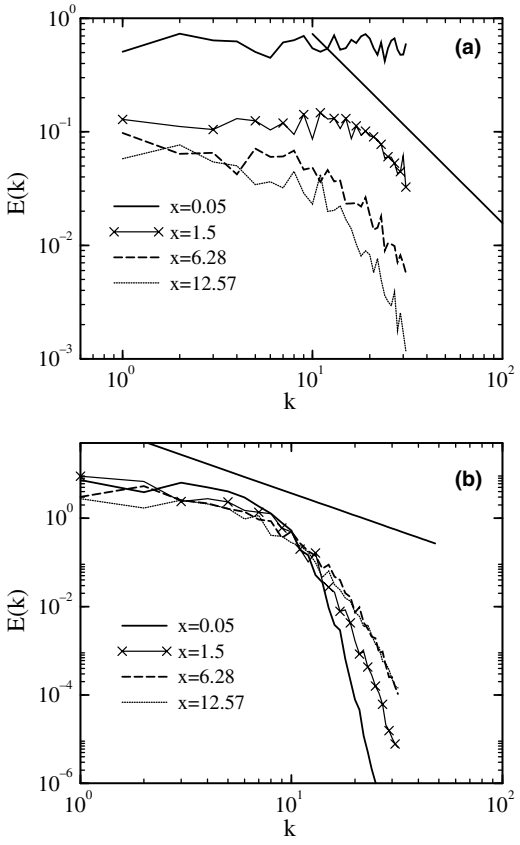

Fig. 3. Development of the longitudinal one-dimensional energy spectrum for the spatially decaying isotropic turbulence. (a) Calculation RAND, (b) Calculation SEM0.

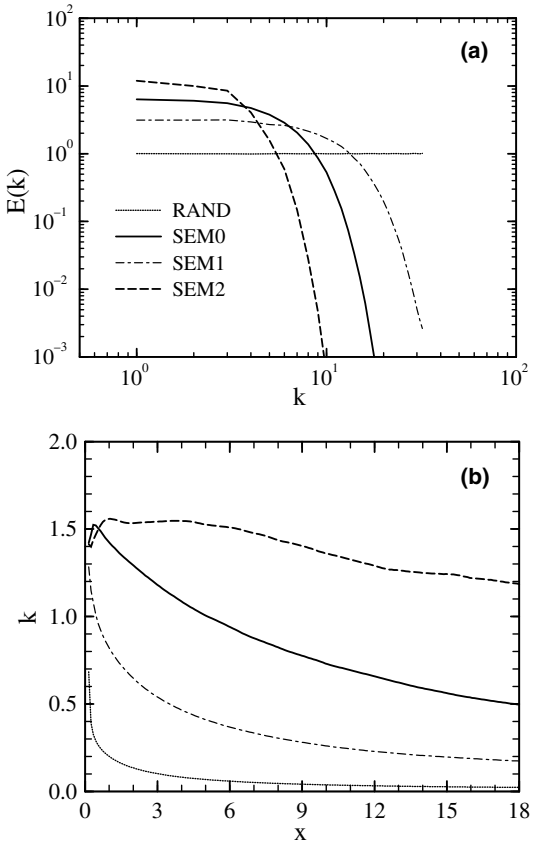

Fig. 4. (a) One-dimensional longitudinal energy spectrum of the inflow data and (b) downstream evolution of the turbulent kinetic energy for spatially decaying isotropic turbulence.

ated, the inflow data becomes less and less correlated, the dissipation increases and the decay rate tends towards the decay rate of RAND.

4. Plane channel flow

The quality of a synthetic turbulent inlet methodology is measured by its capacity to maintain and/or produce self-sustaining turbulence after the shortest possible development period. The theoretical distance of development after which a laminar flow entering a channel is considered as fully turbulent is more than 110δ where δ is the channel half width. It was reported (Le et al., 1997) that about 10δ were needed to recover correct intensity levels for a DNS of a turbulent boundary layer with an inflow data generated with a spectral method.

The chosen Reynolds number of $Re^* = 395$ for this test case, in combination with a fairly coarse mesh makes the case more challenging (real LES rather than quasi DNS). The mesh dimensions are $24\delta \times 2\delta \times 3\delta$ (respectively in the x, y and z direction) to allow a fully developed flow to establish from the inlet. The number of cells is $160 \times 30 \times 30$ and $\Delta x^+ = 60$, $\Delta y^+_{\text{mean}} = 24$, $\Delta y^+_{\text{min}} = 1$, $\Delta z^+ = 40$. Periodic boundary conditions are used in the spanwise direction and a no-slip boundary condition is used at the walls. The Smagorinsky constant is set to its recommended value ($C_S = 0.065$) with Van Driest near-wall damping. Simulations carried out using different inflow data are listed in Table 2.

Table 2
Computations for the turbulent channel flow case at $Re^* = 395$

Computation	Method	Details
PREC	Prec calculation	X
RAND	Basic random	X
SPEC	Spectral method	$\kappa^2 e^{-(\kappa/\kappa_0)^2}, L = 0.4$
SEM0	SEM	Gaussian spots, $L = 0.4$
SEM1	SEM	Gaussian spots, $L = 0.8$
SEM2	SEM	Gaussian spots, $L = 0.2$
SEM3	SEM	$\overline{u_i u_j} = 2/3k\delta_{ij}, L = k^{3/2}/\varepsilon$

The precursor simulation PREC uses periodic boundary conditions in the streamwise direction. It was carried out on a domain of dimensions $6\delta \times 2\delta \times 3\delta$. The mesh is the same as the one used for the spatially developing flow in order to avoid interpolation at the interface. Velocity fields from a plane perpendicular to the mean flow were stored and injected at the inlet of the spatially developing simulation. The basic random procedure RAND generates series of independent random numbers at each point of the inlet mesh at each time step. SEM0 uses the SEM with 3D isotropic spots of constant size across the domain. As a first

approximation the radius of the spot is chosen as $\sigma = 2\Delta z$ (hence $L = 2\sigma = 4\Delta z = 0.4$). The synthetic eddies are convected by the bulk velocity U_B in Eq. (5). The spectral method of Lee et al. (1992) with a constant Gaussian spectrum across the flow is used at the inflow for SPE0. The spectrum is chosen so that SEM0 and SPE0 produce inflow data with the same integral length scale. All the simulations use the same mean velocity and Reynolds stresses profiles obtained from the periodic calculation.

Calculation PREC is used as a baseline for comparison with other methods. Fig. 5 shows the downstream evolution of isoprofiles of $Q = \Omega^2 - S^2$ and Fig. 6 the evolution of the friction coefficient. As expected PREC does not produce any transient downstream of the inlet. On the contrary the intensity of the fluctuations imposed with the basic random procedure at the inlet of RAND seems to decay and the friction coefficient decreases which shows that the flow tends to laminarize. The basic random method does not manage to produce self-sustaining turbulence for this case. It can be seen on Fig. 5 that the SEM succeeds in generating large scale eddies which are sustained downstream of the inlet. The evolution of the skin friction coefficient (Fig. 6) and of the Reynolds stresses (Fig. 7) give more insight into the evolution of the turbulence downstream of the inlet for SEM0. The skin friction decreases up to $x = 3\delta$ where it reaches a minimum. This is caused by a drop of the levels of intensity of all the Reynolds stresses. Then realistic correlations and structures establish which enhance the mixing of momentum at the wall. The skin friction increases again and reaches its fully developed initial value by the end of the domain. The same behaviour can be observed for SPEC. The large scale structures introduce at the inlet of SEM0 and SPEC manage to evolve towards realistic structures specific to the flow after a transition period where they adapt to the Navier–Stokes

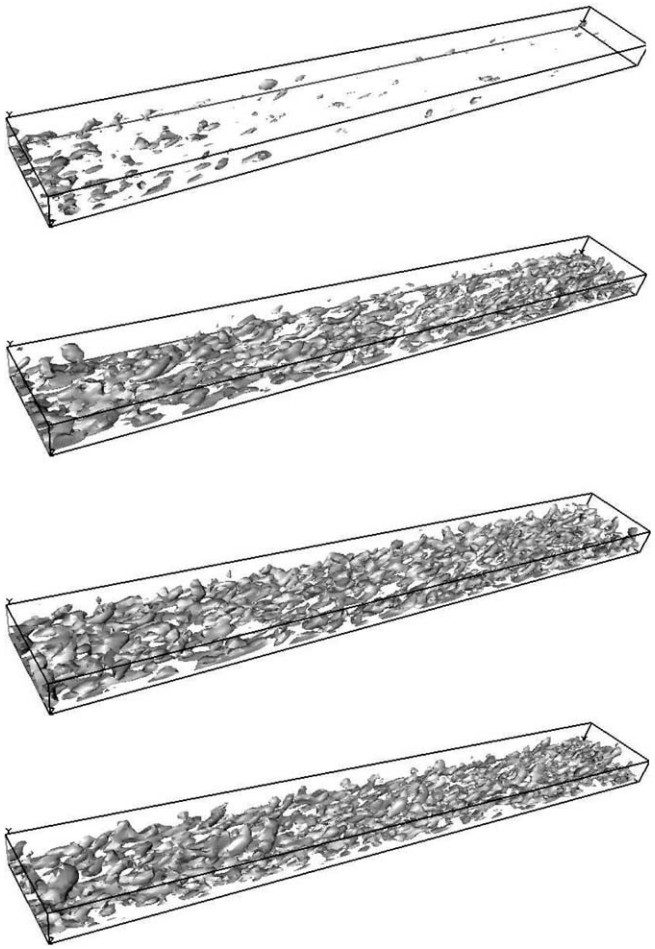

Fig. 5. Isoprofiles $Q = 3$ for the plane channel flow using different inflow generation methods. From top to bottom computation RAND, SEM0, SPEC and PREC.

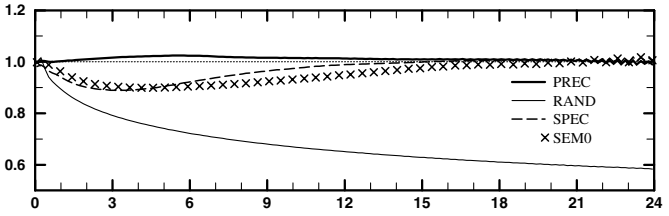

Fig. 6. Downstream development of the friction coefficient at the bottom wall for the channel flow case using different inflow generation methods.

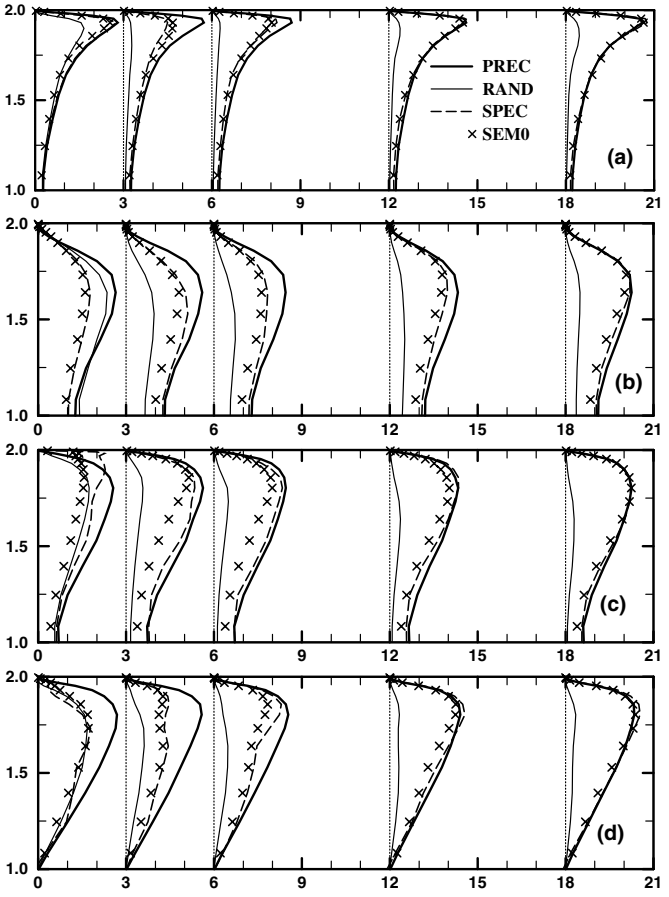

Fig. 7. Downstream development of the Reynolds stresses profiles on the top half of the channel for different inflow generation methods, (a) $x + \overline{u^2}/3.5$, (b) $x + \overline{v^2} \times 4$, (c) $x + \overline{w^2} \times 2.2$ and (d) $x + \overline{uv} \times 3.5$.

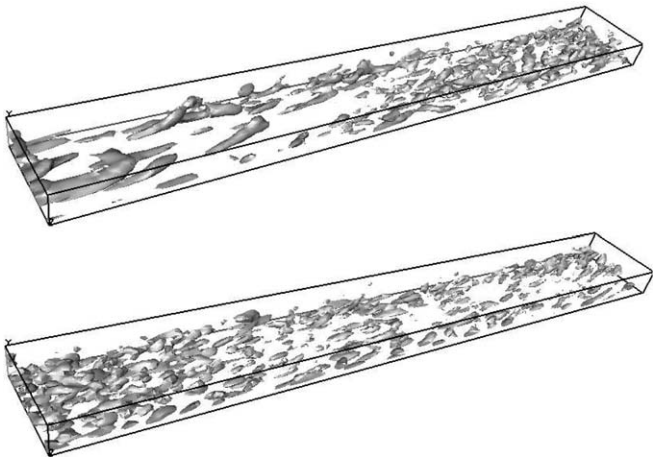

Fig. 8. Isoprofiles $Q = 3$ for the plane channel flow using the SEM with different sizes of eddies. Computation SEM1 (top) is with eddies larger than in the reference calculation SEM0, computation SEM2 (bottom) is with smaller ones.

equations and the numerical scheme and by the end of the domain we have fully developed turbulence.

Different sizes of eddies will now be tested to try to reduce the development section. Fig. 8 shows isoprofiles of Q for the larger SEM1 and smaller SEM2 inlet structures. SEM2 has structures of the size of the structures of the real flow at the wall, whereas SEM1 has structures of the size of the real flow in the middle of the channel. The structures generated with SEM2 seem too small to generate fully developed turbulence by the end of the domain. These tend to decay rather than to evolve towards larger scales. On the contrary SEM1 starts with too large structures but in the second half of the channel these are seen to adapt (or possibly generate new structures) with correct length scales. This confirms the results obtained in isotropic turbulence where energy at low wavenumbers is more easily cascaded into high wavenumbers than the opposite. The evolution of the friction coefficient is given on Fig. 9. The large scale structures generated at the inlet of SEM1 are not adapted to the flow at the wall and the drop in the friction coefficient is more important than for SEM0. However by the end of the domain the large eddies finally manage to break up into suitable structures for the flow and the friction recovers its initial value. Fig. 10 shows the evolution of the Reynolds stresses downstream of the inlet for SEM0,

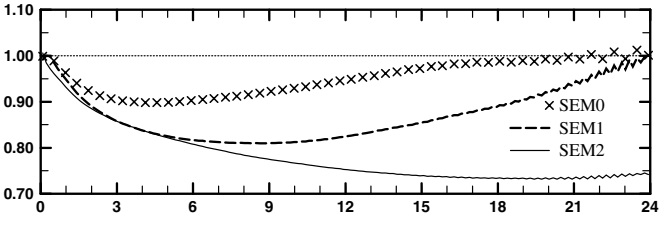

Fig. 9. Downstream development of the friction coefficient $c_f(x)/c_f(0)$ at the bottom wall of the channel for different sizes of eddies.

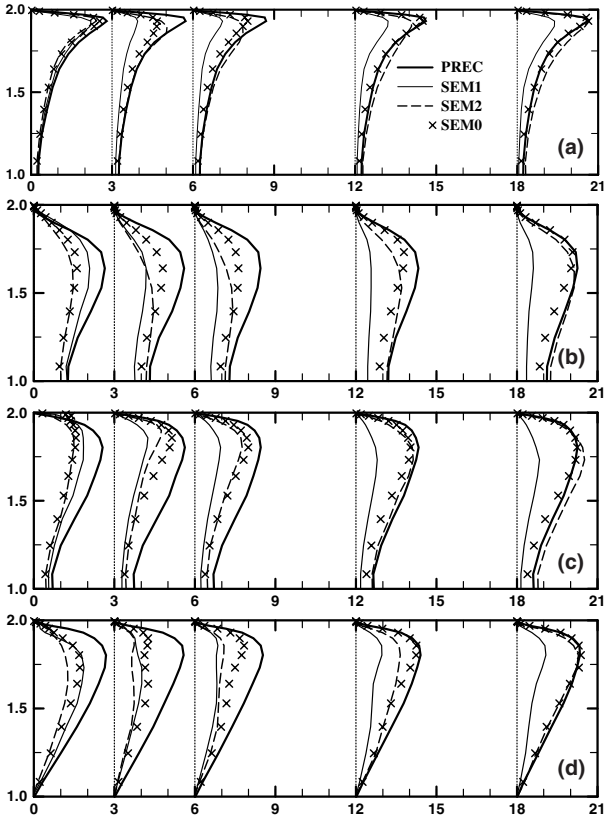

Fig. 10. Downstream development of the Reynolds stresses profiles downstream the inlet on the top half of the channel $Re^* = 395$ for different sizes of eddies (a) $x + \overline{u^2}/3.5$, (b) $x + \overline{v^2} \times 4$, (c) $x + \overline{w^2} \times 2.2$ and (d) $x + \overline{uv} \times 3.5$.

SEM1 and SEM2. All the stresses on Fig. 10 are vanishing towards the end of the domain for SEM2. It can be seen that all the stresses reach fully developed turbulence levels at the wall faster for SEM0 than for SEM1. On the contrary, the structures in the middle of the channel of SEM0 are smaller than those of SEM1 so they are dissipated faster and SEM0 lacks energy in the middle of the channel. This stresses the importance of having different sizes of structures in different regions of the flow.

Finally, a calculation using only RANS information is used. A $k-\varepsilon$ calculation of the channel flow at $Re^* = 395$ is run and profiles of k and ε from this calculation are used as the only source of information for the SEM. Instead of the resolved Reynolds stress tensor obtained from the periodic LES, the model Reynolds stress tensor obtained from the $k-\varepsilon$ calculation is used $\overline{u_i u_j} = 2/3k\delta_{ij} - 2\nu_t \overline{S}_{ij}$. The size of the structures is calculated using a turbulent length scale $k^{3/2}/\varepsilon$. In order for the synthetic eddies to be properly discretized by the inlet mesh, the radius of the eddies reads $\sigma = \max(\Delta z,\ k^{3/2}/\varepsilon)$. On Fig. 11(a) the downstream evolution of the friction coefficient shows a very short transient and an error of less than 5% is attained after only 3δ. This value even increases just downstream of the inlet. This can be explained by the higher value of the wall-normal Reynolds stress $\overline{v^2}$

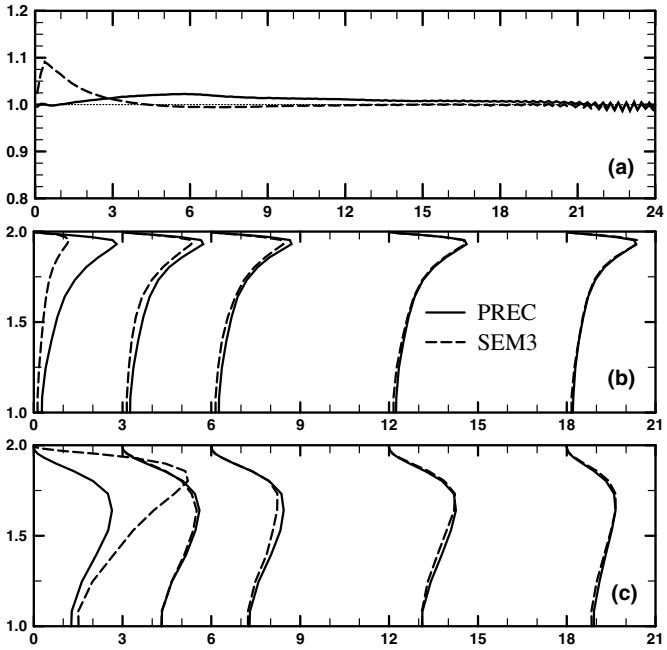

Fig. 11. Downstream development of (a) the friction coefficient $c_f(x)/c_f(0)$ at the bottom wall of the channel, (b) $x + \overline{u^2}/3.5$ and (c) $x + \overline{v^2} \times 4$.

generated in SEM3 (as erroneously predicted by the $k - \varepsilon$ model) which strongly enhances the mixing of momentum at the wall. It can be seen on Fig. 11(b) that $\overline{u^2}$ which is underestimated at the inlet reaches fully developed value after only 3δ. The excess of $\overline{v^2}$ at the inlet is quickly dissipated and after 3δ too, the fully developed turbulent profiles are recovered (Fig. 11(c)). The importance of the wall-normal velocity fluctuations has already been stressed by Keating et al. (2004) and Spille-Kohoff and Kaltenbach (2001).

5. Conclusion

A new method for generating turbulent inlet boundary conditions has been developed and compared to existing methods on two test cases. The method generates synthetic eddies on the inlet plane. Each eddy is represented by a specific shape function which describes its spatial and temporal characteristics. The method is able to reproduce specific first and second order one point statistics as well as autocorrelation functions.

Compared to the random method, the new approach can produce spatial and temporal correlations which produce fully developed turbulence in a channel flow a few diameters downstream of the inlet. It gives similar results to the spectral method of Lee et al. (1992) for the two test cases computed but is more appropriate for complex geometries on unstructured mesh.

The importance of the size of the structures at the inflow has been shown both on the isotropic turbulence and on the channel test case. It appears to be essential to generate inflow structures which can be properly discretized by the inlet mesh even if it means overestimating their size.

The generation of synthetic turbulence with reduced information coming from a RANS simulation gives a very short transition section downstream of the inlet for the channel flow case and allows us to use very short domains, thus reducing the computational cost. the synthetic-eddy-method is therefore very promising to force synthetic turbulence at the interface of a hybrid RANS/LES flow solver. The method is currently being extended to represent turbulence generation parallel to the wall for RANS/LES simulations of high Reynolds number channel flows on coarse grids.

Acknowledgements

The work was partially supported by the EU project DESider, which is a collaboration between Alenia, ANSYS–AEA, Chalmers University, CNRS–Lille, Dassault, DLR, EADS Military Aircraft, EUROCOPTER Germany, EDF, FOI–FFA, IMFT, Imperial College London, NLR, NTS, NUMECA, ONERA, TU Berlin, and UMIST. The project is funded by the European Community represented by the CEC, Research Directorate–General, in the 6th Framework Programme, under Contract No. AST3-CT-2003-502842.

References

Archambeau, F., Mehitoua, N., Sakiz, M., 2004. Code saturne: a finite volume code for the computation of turbulent incompressible flows. International Journal on Finite Volumes 1 (1).

Batten, P., Goldberg, U., Chakravarthy, S., 2004. Interfacing statistical turbulence closures with large-eddy simulation. AIAA Journal 42 (3), 485.

Benhamadouche, S., Laurence, D., 2003. LES, coarse LES, and transient RANS comparisons of the flow across a tube bundle. International Journal of Heat and Fluid Flow 24, 470–479.

di Mare, L., Jones, W.P. 2005. Algebraic and operators methods for generation of inflow data for LES and DNS, TSFP4. In: 4th International Symposium on Turbulence and Shear Flow Phenomena, vol. 2, Williamsburg, VA, USA, pp. 687–692.

Druault, P., Lardeau, S., Bonnet, J.-P., Coiffet, F., Delville, J., Lamballais, E., Largeau, J.-F., Perret, L., 2004. Generation of Three-Dimensional Turbulent Inlet Conditions for Large-Eddy Simulation. AIAA Journal 42 (3), 447.

Jarrin, N., Benhamadouche, S., Addad, Y., Laurence, D. 2003. Synthetic turbulent inflow conditions for large eddy simulation. In: Proceedings, 4th International Turbulence, Heat and Mass Transfer Conference, Antalya, Turkey.

Kaltenbach, H.-J., Fatica, M., Mittal, R., Lund, T.S., Moin, P., 1999. Study of flow in a planar asymmetric diffuser using large-eddy simulation. Journal of Fluid Mechanics 390, 151–185.

Keating, A., Piomelli, U., Balaras, E., Kaltenbach, H.-J., 2004. A priori and *a posteriori* tests of inflow conditions for large-eddy simulation. Physics of Fluids 16 (12), 4696–4706.

Klein, M., Sadiki, A., Janicka, J., 2003. A digital filter based generation of inflow data for spatially developing direct numerical or large eddy simulations. Journal of Computational Physics 186, 652–665.

Kondo, K., Murakami, S., Mochida, A., 1997. Generation of velocity fluctuations for inflow boundary conditions of LES. Journal of Wind Engineering and Industrial Aerodynamics 67&68, 51–64.

Le, H., Moin, P., Kim, J., 1997. Direct numerical simulation of turbulent flow over a backward-facing step. Journal of Fluid Mechanics 330, 349–374.

Lee, S., Lele, S., Moin, P., 1992. Simulation of spatially evolving compressible turbulence and the application of Taylors hypothesis. Physics of Fluids, 1521–1530.

Lund, T., Wu, X., Squires, D., 1998. Generation of turbulent inflow data for spatially-developing boundary layer simulations. Journal of Computational Physics 140, 233–258.

Smirnov, A., Shi, S., Celik, I., 2001. Random flow generation technique for large eddy simulations and particle-dynamics modeling. Journal of Fluids Engineering 123, 359–371.

Spille-Kohoff, A., Kaltenbach, H.-J. 2001. Generation of turbulent inflow data with a prescribed shear-stress profile. In: Liu, C., Sakell, L., Beutner, T. (Eds.), Third AFOSR International Conference on DNS/LES Arlington, TX, 5–9 August 2001, DNS/LES Progress and Challenges. Greyden, Colombus, OH.